Геология и геофизика, *т. 65, № 9, с. 1289—1301,* DOI: 10.15372/GiG2024119, EDN: USWXVH
Поступила в редакцию 04.07.2023, принята в печать 29.03.2024 *Опубликована онлайн: 01.04.2024*

УДК

ХАРАКТЕР ЗАЛЕГАНИЯ ОТ ИСТОЧНИКА К ОТЛОЖЕНИЮ ГОРИЗОНТА ШАХЭЦЗЕ НА СКЛОНЕ ШУЛУ (*бассейн залива Бохай, Китай*)

Л. Лю[1], Ц. Лю[1], Ж. Чжао[2], С. Ли[3], С. Ли[4], С. Ло[1], Л. Чжао[5,6], Т. Лю[7]

[1] *School of Earth Sciences, Northeast Petroleum University, Daqing, Fazhan Rd., No. 184, 163318, China*

[2] *School of Earth Sciences, Jilin University, Changchun, Jianshe St., No. 2199, 130061, China*

[3] *Exploration Division of HuaBei Oilfield Company, RenQiu city, Huizhan Rd., North China Oilfield Hotel south, 062552, China*

[4] *Exploration and Development Research Institute of HuaBei Oilfield Company, RenQiu city, Jianshe Middle Rd., No. 1, 062552, China*

[5] *Research Center for Computational and Exploration Geophysics, Chinese Academy of Sciences, Wuhan, 430077, China*

[6] *University of Chinese Academy of Sciences, Beijing, YuQuan, No. 19, 100049, China*

[7] *School of Computer and Information Technology, Northeast Petroleum University, Daqing, Fazhan Rd., No. 99, 163318, China*

Эрозия и осадочные формы рельефа связаны между собой путями переноса отложений, которые образуют систему источник—отложение (S2S). Концепция S2S подчеркивает взаимосвязь различных компонентов в системе обломочных отложений. Также предлагается новый метод характеристики осадочного процесса в континентальных рифтовых бассейнах. Доказано, что третья пачка горизонта Шахэцзе (Es_3) на склоне Шулу в бассейне залива Бохай в Китае обладает богатым потенциалом для разведки, но при относительно низкой добыче. Учитывая сложную структуру Es_3 на склоне Шулу, традиционные методы исследования неэффективны при разработке текущих стратегий освоения. Таким образом, в данной работе применяется теория S2S, а элементы системы характеризуются с использованием данных керна, каротажа и сейсморазведки. Результаты показывают, что S2S в этом исследуемом районе была обеспечена поднятием Нинцзинь в западном регионе, а конус выноса и озерные осадочные системы были сформированы песком, перенесенным через долины и приразломные впадины. Разработана модель взаимосвязи S2S: «Поднятие Нинцзинь, источник песка — приразломная впадина, перенос в долину — конус выноса и осаждение на мелководье озера». Эта область исследований позволяет прогнозировать песчаные тела в континентальных рифтовых бассейнах со сходным структурным фоном.

Озерный рифтовый бассейн, система «источник — отложение», осадочные характеристики, Es_3, склон Шулу

THE SOURCE-TO-SINK CHARACTER OF THE SHAHEJIE FORMATION IN THE SHULU SLOPE (*Bohai Bay Basin, China*)

L. Liu, Z. Liu, R. Zhao, X. Li, X. Li, X. Luo, L. Zhao, T. Liu

Erosion and sedimentary landforms are linked through sediment transport pathways, which forms a source-to-sink system (S2S). The coupling relationship of different components in the clastic sediment system is emphasized by the S2S concept. A new method for characterizing the sedimentary process of continental rift basins is also provided. It has been proven that there is rich exploration potential in the third member of the Shahejie Formation (Es_3) in the Shulu Slope of the Bohai Bay Basin in China but with relatively low production. With the complex structural background of the Es_3 of the Shulu Slope, conventional research methods are ineffective in guiding the current development strategies. Therefore, this study adopts the S2S theory, and its elements in the study are characterized using core, logging, and seismic data. The results suggest that the S2S in this study area was supplied by the Ningjin Uplift in the western region, and a fan delta and lake sedimentary systems were formed by the sand transported through valleys and fault troughs. The S2S coupling model, "the Ningjin Uplift sand supply–fault trough, valley transport–fan delta, and shore–shallow lake sedimentation," is established. This research field permits prediction of sand bodies in continental rift basins with similar structural backgrounds.

Lacustrine rift basin, source-to-sink, sedimentary characteristics, Es_3, Shulu Slope

INTRODUCTION

Rift basins are a significant source of oil and gas resources, accounting for approximately one-third of global reserves, and, thus, have always been of interest to the petroleum industry (Tian et al., 2023). Rift basins form during the process of lithosphere stretching and thinning and are characterized by long, narrow boundaries

✉e-mail: lzbdqpi@163.com

composed of normal faults and thinning crusts. These modes of continental extension can be categorized depending on the width and deformation mechanism of the rift, namely, narrow rift mode, wide rift mode, and core composite mode (Wang et al., 2022). By understanding these modes, we can gain a better understanding of how rift basins form and how to best explore and exploit their resources. Lacustrine rift basins, such as the offshore Bohai Bay Basin (OBBB) in eastern China, are characterized by diverse sedimentary sources and complex filling (Li et al., 2023; Paisani et al., 2023; Ribeiro et al., 2023; Zhao et al., 2023), which correspond to different stages in the evolution of each particular basin (Peng, 2018; Savelyev et al., 2018; Liu et al., 2020; Cuitiño et al., 2023).

Within a rift basin, the slope encompasses approximately 50% of the total area and is highly significant for the migration and accumulation of oil and gas resources (Zhao et al., 2016; Liang et al., 2020), since it generally develops of multiple sedimentary facies, including the fluvial, delta, and shallow lake facies (Zhu et al., 2022). The slope zone of a rift lacustrine basin is not only a sediment deposition area but also a sediment transport channel, which has a significant impact on the sediment distribution. Typically, slope zones in lacustrine rift basins can be categorized as either steep or gentle slopes, depending on their gradients. Each is characterized by complexity and diversity and influenced by factors, such as tectonic activity, which play a significant role in shaping the depositional environment and processes. In the past decade, research on the slopes of rift lacustrine basins has focused generally on the rift style, sequence stratigraphy, and the diffusion model of lacustrine marginal sediments, thus laying a foundation for the analysis of sedimentary environments and the prediction of the properties of reservoirs (Liu et al., 2020; Devyatov and Nikitenko, 2023; Kosenko et al., 2023; Travin et al., 2023; Polyansky et al., 2024).

However, slope types are rarely considered in this study of the source-to-sink system (S2S) of faulted lacustrine basins, and the study of the S2S steep slope with complex structural characteristics is particularly weak. The width and slope of the strata are common geometric features of the slope zone, which can directly reflect its genetic mechanism and sedimentary structure characteristics and are an important basis for the classification of slope types. According to the previous slope classification scheme (Zhao et al., 2016), the average gradient of the Shulu Slope is a typical steep slope. Continental rift basin steep slope belts are widely developed in the world, such as the steep slope area of the Jiyang Depression in the Bohai Bay Basin (Gao et al., 2024), the slope zone of the Ulyastai Depression in the Erlian Basin (Feng et al., 2021), the western slope of the Mahu Depression in the Zhungeer Basin (Xiao et al., 2021), and the steep mountain range area of the Baikal Rift System (Byzov and Sankov, 2024).

Located in the Jizhong Depression in the northwestern part of the OBBB, the Shulu Slope features favorable conditions for the accumulation of oil and gas resources. However, to date little oil–gas exploration has been conducted in this promising area. Thus, it is an important target for the increase of reserves and production in the North China oilfield. This article presents the Shulu Slope as an example for exploring the characteristics of the steep slope coupling mode. The main objectives of this study are threefold: (1) to investigate and characterize the components of the S2S, utilizing the S2S theory as a framework; (2) to elucidate the types and spread patterns of sedimentary systems within the Shulu Slope; and (3) to summarize the coupling mode of the S2S of the Shulu Slope. Moreover, the overall aim of this work is to provide guidance for the prediction of sand bodies with similar geologic backgrounds.

GEOLOGIC SETTING

The OBBB formed on the North China Craton basement in eastern China (Feng et al., 2016; Liu et al., 2019) (Fig. 1). It is rich in oil reserves, and it has a development history of more than 40 years (Feng et al., 2016). The tectonic evolution of the OBBB can be examined within four distinct stages with the Cenozoic considered to be the primary interval for the development of the petroliferous basin, including the Paleogene rifting stage and the Neogene postrift thermal subsidence stage (Liu et al., 2016). The Shahejie Formation (Es) and Dongying Formation (Ed) were established during the Paleogene. These sedimentary formations are especially important, because they are associated with the deposition of organic-rich parental rocks and reservoirs within the OBBB (Fig. 1*e*).

The Shulu Slope, localized in the southern section of the OBBB Jizhong Depression and the western part of the Shulu Depression (Fig. 1*b*), holds considerable significance as a key area for oil and gas exploration. The eastern side is controlled by the Xinhe Fault, while the western side transitions gradually to the boundary of the Ningjin Uplift; the southern part is the Xiaoliucun Uplift; and the northern part is controlled by the Hengshui Fault (Zheng et al., 2015). The Shulu Slope is approximately 43 km long and 10 km wide (Fig. 1*c*) and covers an area of approximately 370 km^2. Its development is determined by the structural events of the Jizhong Depression (Xiang et al., 2021). Three faults formed during the Middle Jurassic to Late Cretaceous Yanshanian orogeny, namely, the Hengshui, Taijiazhuang, and Jingqiu faults, each of which played a crucial role in shaping the topographic features within the basin, dividing it into three areas: north, middle, and south (Tang et al.,

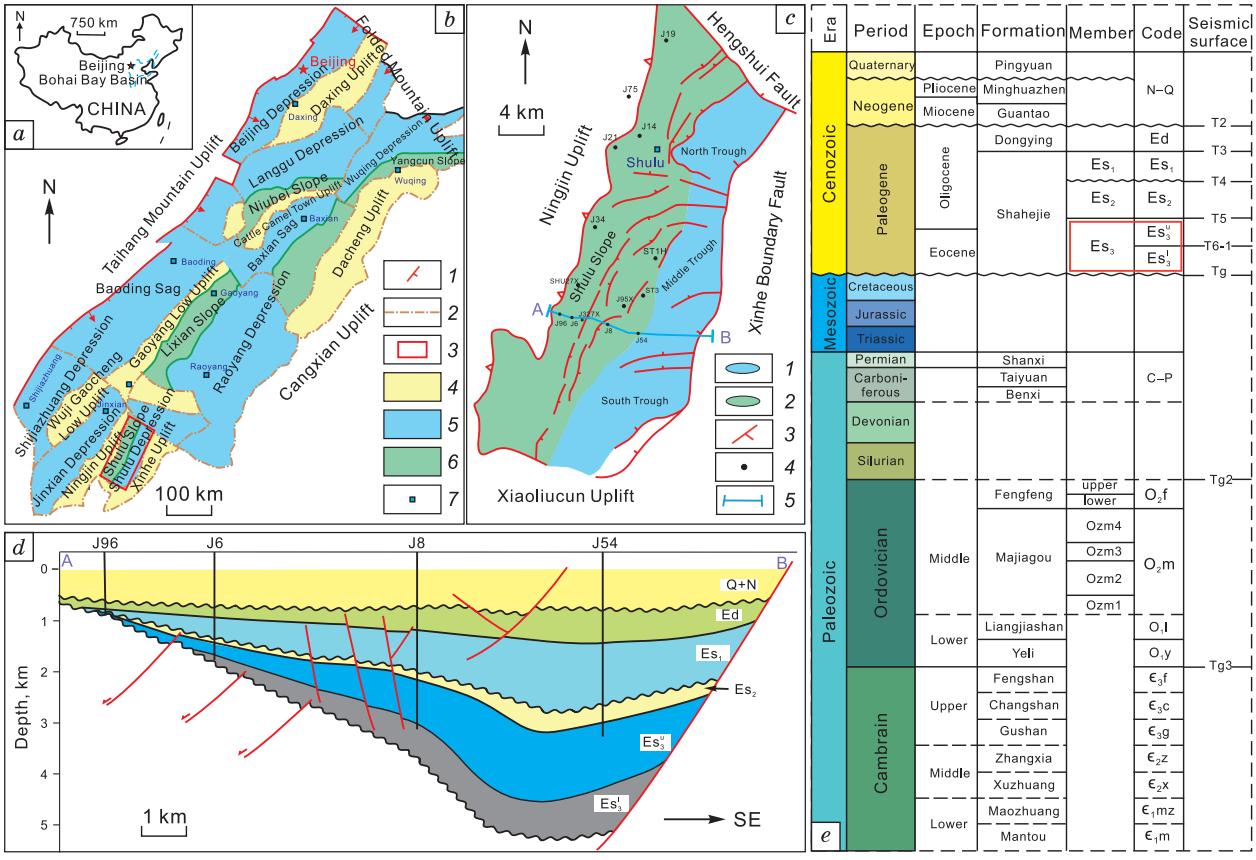

Fig. 1. Regional context: *a* – Location of the offshore Bohai Bay Basin (OBBB) in East China; *b* – tectonic location of the Jizhong Depression in the OBBB, China:

1 – fault; *2* – secondary structural unit; *3* – study area; *4* – uplift area; *5* – depression area; *6* – slope area; *7* – city; *c* – structural map of the Shulu Slope; *d* – cross section and structural unit division of the Shulu Slope (see *c* for location of the cross section); *e* – generalized stratigraphic column of the Shulu Slope with red boxed strata representing the target interval of this study.

2018; Li et al., 2020b). The Shulu Slope Paleogene lacustrine strata lie on top of marine carbonate rock strata from the Cambrian, Ordovician, and Carboniferous–Permian periods. They extend gradually toward the Ningjin Uplift in the west (Kong et al., 2020), which is composed of Cambrian and Ordovician marine carbonate rocks. They are the main parental rocks and control the composition of the basin fillings (Kong et al., 2019a; Li et al., 2020b). From bottom to top, the Shulu Slope develops successively as follows: Jixian Wumishan Formation (JXW), Cambrian System (Є), Ordovician (O), Paleogene Shahejie Formation (Es), Dongying Formation (Ed), Neogene Guantao Formation (Ng), Minghuazhen Formation (Nm), and Quaternary Plain Formation (Qp) strata. The Es Formation is further divided from bottom to top into Es_3, Es_2, and Es_1 (Kong et al., 2019b; Li et al., 2020a), bounded by seismic-interpreted basement units T6, T5, and T4. Es_3 is the main oil-bearing formation, in turn, divided into the upper (Es_3^u) and lower (Es_3^l) submembers (Fig. 1*e*) (Zhao et al., 2014; Cai et al., 2022; Liu et al., 2022). During the sedimentary period of Es_3, the Shulu Slope was dominated by fan delta sedimentation and, consequently, developed carbonate breccia and sandstone reservoirs.

DATA AND METHODS

This research employed seismic and geological data to describe the characteristics of the elements in the S2S system of the Shulu Slope. Additionally, the research outlined the coupling model in the Es_3 formation within this study area. Three-dimensional (3D) seismic, cable logging, and core data provided by PetroChina Huabei Oilfield Company were utilized in determining the sedimentary characteristics of the Es_3 formation. The bandwidth range of the 3D seismic data volume frequency was found to be approximately 0–50 Hz, with a main frequency of around 30 Hz. Logging sequences in this study included mainly GR, SP, and resistivity curves. In the research area, a grand total of 150 wells were drilled; however, only two thin slice photos of the core were collected, which were used to discuss the characteristics of the original rock. The thickness of the rock layer in

a single well was utilized to create a map of the distribution of the stratum thickness. The ancient valleys of Es_3 in the research area were determined based on the two NE–SW seismic profiles that cross the Shulu Slope, and the types and morphology of its sediment transport channels were analyzed and observed from these two seismic profiles. Logging data and lithologic characteristics were used to determine the sedimentary environment of the target stratum in the research area, and a sedimentary microfacies map was generated using root mean square (RMS) amplitude attribute slices. Finally, based on the analysis of the sources, transport channels, and sedimentary environment, an S2S coupling model was established.

RESULTS AND DISCUSSION

Source characteristics. Source analysis was used to ascertain the foundation of sedimentary patterns and sand body distribution, without which a complete S2S system cannot be formed. The Ningjin Uplift is the dominant source area of the Shulu Slope, and, thus, it provided the material basis for the S2S system of the research area.

Based on the seismic data and with reference to previous layered systems, contour maps of the stratigraphic thickness of Es_3^l and Es_3^u were drawn. These revealed that their development was inherited (Fig. 2), with both formations exhibiting features of high landforms in the west and low landforms in the east, indicating that the sediment in the convergence area had entered the study area mainly from the west. The main provenance area of the study area is the western Ningjin Uplift, in line with our previous understanding of the direction from which the Shulu Slope derives.

Lithologic characteristics. The main types of bedrock in the Ningjin Uplift are dolomite and limestone, while the main rock types in the Es_3 formation of the Shulu Slope are argillaceous limestone and dolomitic limestone. The lithology of the Es_3 formation in the Shulu Slope is similar to that in the Ningjin Uplift area.

The Mesozoic bedrock of the Ningjin Uplift consists mainly of large-scale dolomite and limestone formations, serving as the basement. The J75 well is situated in the northern part of the Ningjin Uplift, and its bedrock is composed primarily of gray-white dolomite with a layered agglomerate structure, formed by algal activity in the sediment. In contrast, the J19 well, located in the northern part of the slope, contains mainly argil-

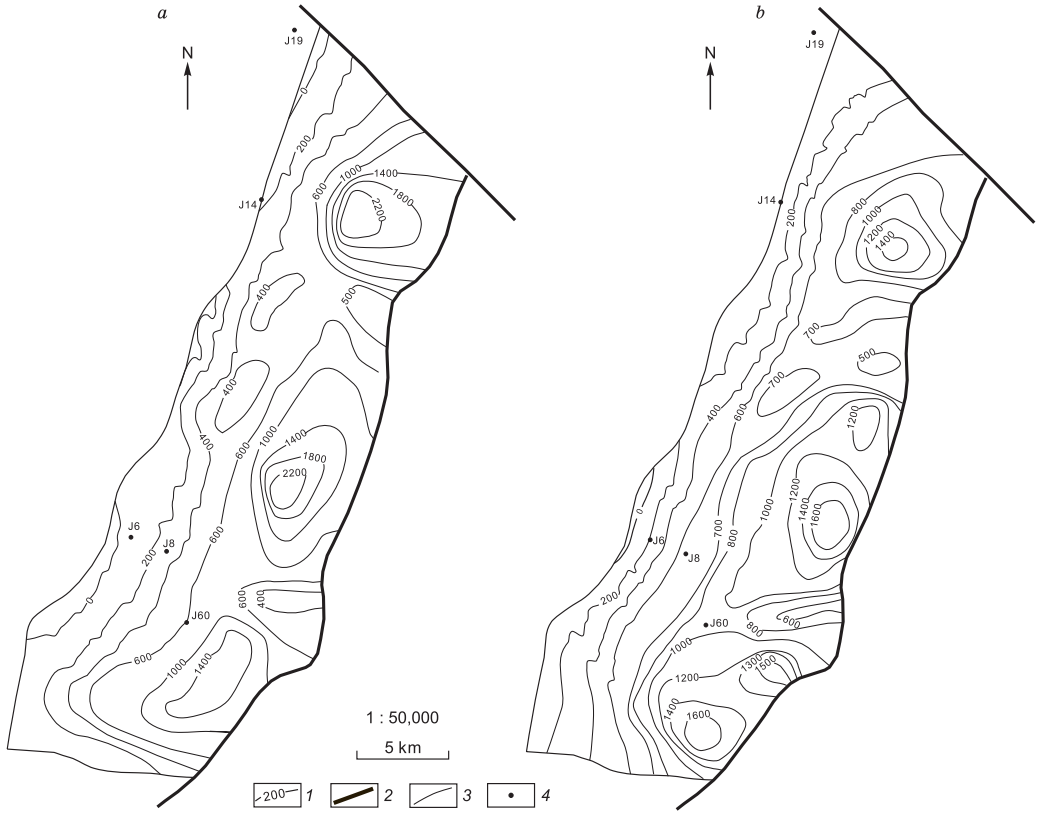

Fig. 2. Stratigraphic thickness contour maps.

a – Stratigraphic thickness distribution of Es_3^l; *b* – stratigraphic thickness distribution of Es_3^u: *1* – thickness contour; *2* – fault; *3* – boundary; *4* – well. The numbers on the pictures are labeled as the stratigraphic thickness in the time domain.

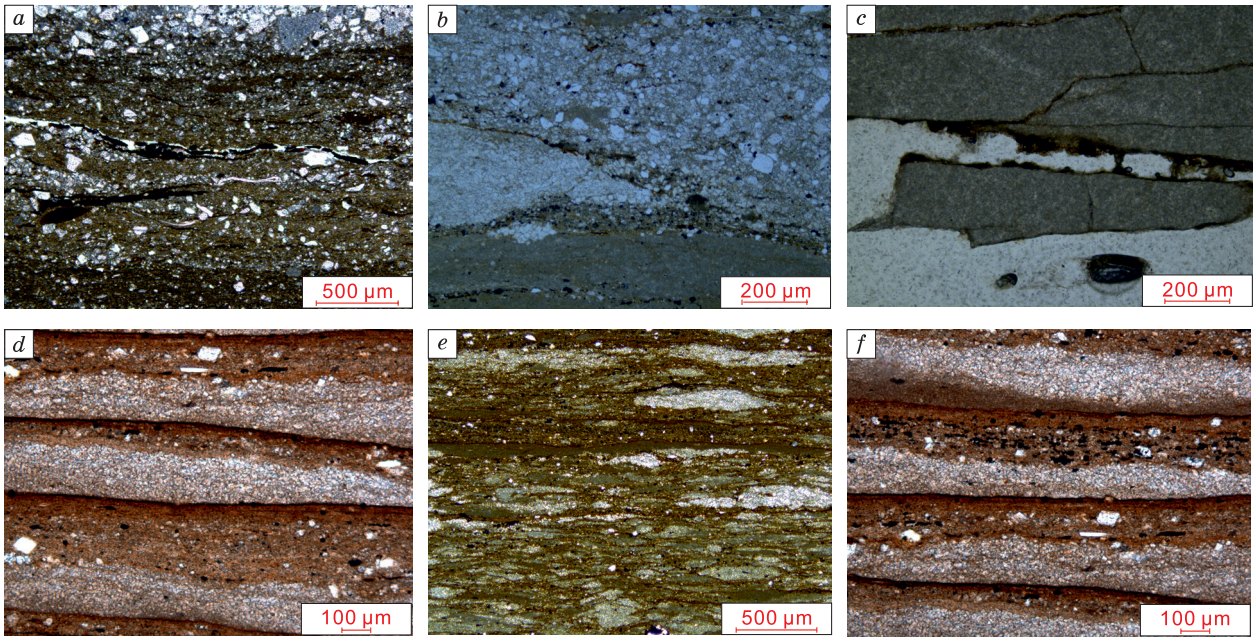

Fig. 3. Micrograph image of bedrock in the Shulu Slope.

a – Laminated gravelly limestone, 3895.76 m; *b* – massive marl, 4096.2 m; *c* – massive gravelly marl, 4315.2 m; *d* – laminated micrite limestone, 4211.5 m; *e* – laminated gray argillaceous limestone, 4212.2 m; *f* – laminated dark gray marl, 4212.7 m.

laceous limestone. Some oolites exhibit a spherical shape and have undergone metasomatism, resulting in recrystallized dolomite, while others are composed of microcrystalline calcite, indicating the influence of late thermal metamorphism. The J34 well, located in the central part of the Ningjin Uplift, contains bedrock that consists of fine-grained crystalline dolomite.

Limestone and argillaceous limestone, which are the major types of bedrock in the Es_3^1 formation, were found to be distributed extensively across the entire region. Among them, ST3 (Fig. 3*a*) on the left side of the middle trough in the Shulu Slope belt begins at a depth of 3895.76 m with grainy-bedded limestone that exhibits a gravel structure, with an argillaceous matrix and calcite distributed between the grains. At a depth of 4096.2 m, a massive formation of marlstone was identified (Fig. 3*b*).

The rock composition of the Shulu Slope is primarily argillaceous calcite with a small amount of silty dolomite, displaying a weak lamellar structure. The sandstone debris components at 4315.2 m (Fig. 3*c*) have relative stability and further reflect the characteristics of the bedrock of the Shulu Slope. Mudstone limestone is mainly developed in ST1H, generally composed of calcite and argillaceous material, with local bedding fractures and pores filled with organic matter (Fig. 3*d–f*).

Continental rift basins are often accompanied by volcanic activities due to active tectonic movements. The volcanic hydrothermal material generated by volcanic activity not only compensates for the concentration

Table 1. **Parameters of the Shulu Slope valley**

Valley	Valley depth, m	Valley width, m	Cross-sectional area, m^2	Transport competence
V1	10.62	90.40	480.02	moderate
V2	5.24	156.49	410.00	moderate
V3	20.50	204.88	2100.02	powerful
V4	10.32	100.78	520.02	powerful
V5	14.60	42.47	310.03	moderate
V6	22.80	45.61	519.95	powerful
V7	19.20	13.54	129.98	weak
V8	10.65	97.65	519.98	powerful
V9	27.50	182.17	2504.84	moderate
V10	8.56	165.99	710.44	moderate
V11	30.50	271.73	4143.88	moderate

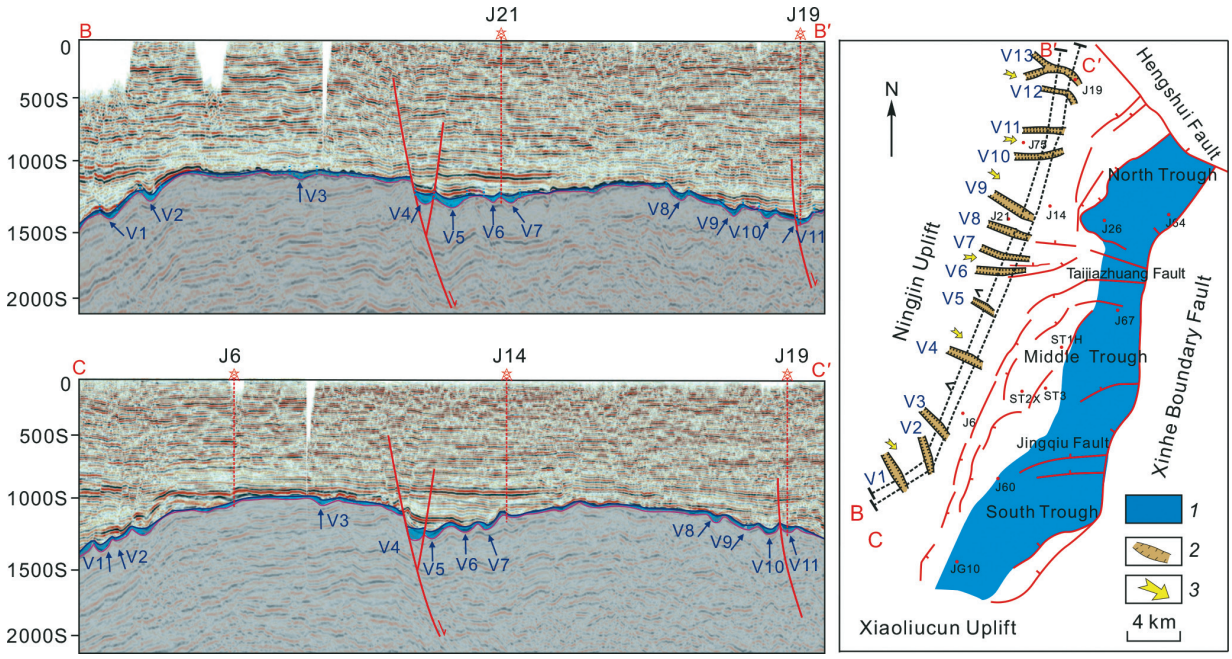

Fig. 4. Distribution of valleys in the Es_3 of the study area:

1 – trough; *2* – paleovalleys; *3* – direction of source.

of SO_4^{2-}, CO_3^{2-}, Ca^{2+}, Mg^{2+}, and other ions in the formation water near the fault and the holes of spring but also increases the crystallization temperature and promotes the formation of nutrient-rich lake basins (Kong et al., 2017; Liu et al., 2021a,b; Bergal-Kuvikas et al., 2023; Eliseev et al., 2024; Nemova et al., 2024; Velivetskaya et al., 2024). The Shulu Slope is controlled by the carbonate source, and the Ningjin Uplift on the west side of the Shulu Slope is the main source area of the study area (Jiang et al., 2021).

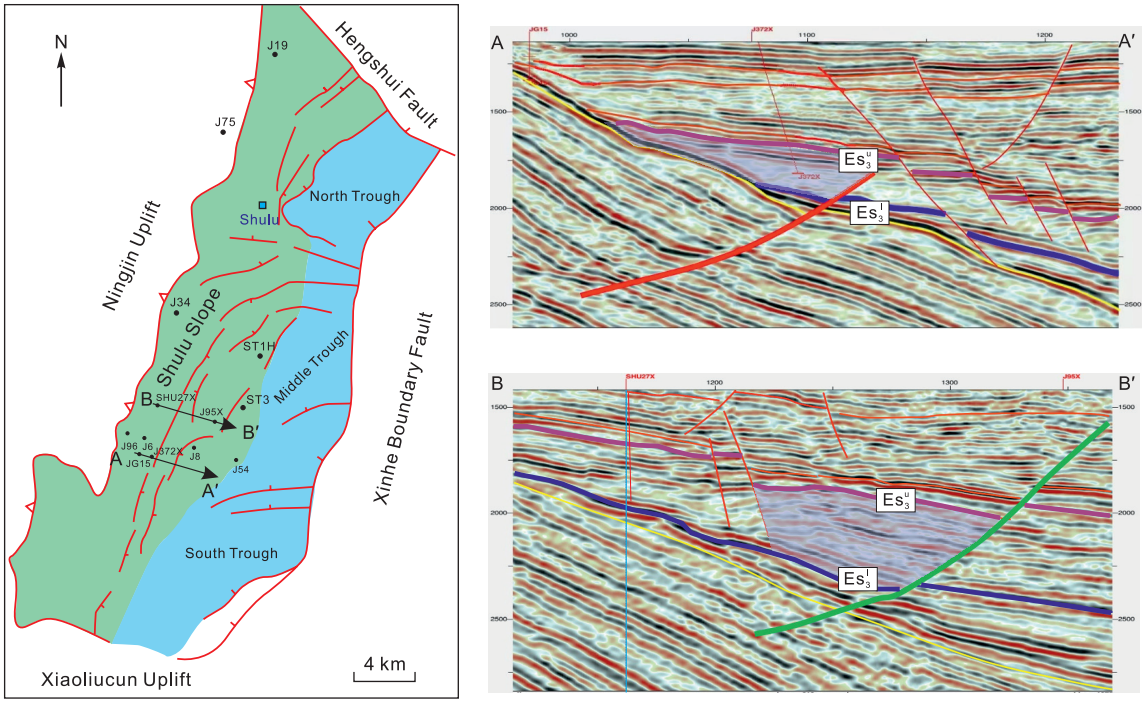

Fig. 5. Distribution of fault troughs in the Es_3 of the Shulu Slope.

The left figure shows the plane position of the seismic profile; the blue solid line on the seismic profile represents the top interface of Es_3^l; the purple solid line represents the top interface of Es_3^u; the red solid line represents the fault formed before sedimentation; the green solid line represents the fault layer formed after sedimentation; and the transparent purple polygon represents the fault groove.

Sediment transport system. The sediment transport system, or channel (Liu et al., 2017), serves as a link between the source area and the sediment area. It is a key factor in shaping the erosion and sedimentary landforms of different sections and serves as a record of the geologic history of an area. In this study area, two modes of sediment transport were identified, namely, ancient valleys and fault troughs, with the sand body distribution most significantly influenced by the valleys.

Ancient valleys. Ancient valleys can be referenced to not only determine the direction of material sources but also predict the planar distribution of sand bodies. They form through surface erosion that occurs once the base level falls beneath the point where the slope changes. As the lake level rises, hydrodynamic forces weaken, and the erosion gullies are filled with terrigenous debris, forming paleovalleys. These paleovalleys serve as important channels for source transport, with their planar distribution indicating the direction of water flow and sediment extension. Additionally, valleys play a crucial role in the control of sedimentary systems and the distribution of sand bodies. The characterization of ancient valleys is, thus, an effective method for clarifying the direction of source supply and the distribution patterns of sediment transport.

Eleven valleys were identified in the Es_3 of the research area (Table 1, Fig. 4). Analysis of their depths, widths, and cross-sectional areas revealed that V7 has the smallest cross-sectional area and the weakest carrying capacity among them. The cross-sectional areas of V1, V2, V5, V9, V10, and V11 were found to range from 0.03 to 0.05 km^2, indicating moderate carrying capacity, while the cross-sectional areas of V3, V4, V6, and V8 are relatively large, reflecting strong handling capabilities.

Fault troughs. Fault troughs are another major pathway for the transportation of sediment in this study area. Relatively low-lying troughs or valleys develop under the influence of one or two adjacent main normal faults. The development of the fault troughs in the J6 well in the Es_3^u unit has had a controlling effect on the distribution of sandstone bodies. At the early stage of development, synsedimentary fault troughs were first filled and then tilted, with the internal in-phase axis nearly parallel and at an angle to the bottom boundary. This controlled the direction of the reservoir sandstone body. At the late stage, nonsedimentary fault troughs were first deposited, then tilted and staggered, with the same phase axis near the top and bottom interfaces, which did not control the reservoir sand body (Fig. 5).

Depositional system. The Shahejie Formation, composed of fan deltas and shallow lake deposits, is a key oil reservoir in the Shulu Slope. To gain a clearer comprehension of the spatial arrangement of sand deposits, an RMS amplitude attribute slice was extracted from the Es_3^l and Es_3^u units as a reference for the identification of sand bodies.

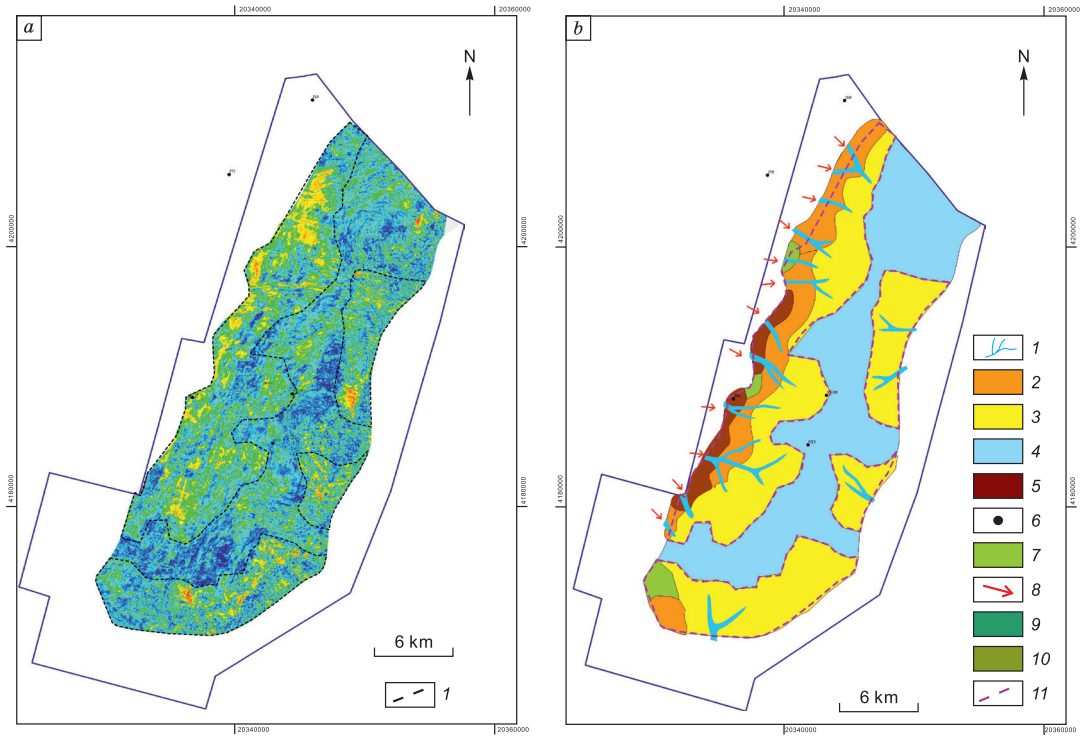

Fig. 6. Sedimentary distribution map of Es_3^l.

a – RMS amplitude attribute slice of the Es_3^l formation: *1* – fan boundary; *b* – sedimentary microfacies distribution map of the Es_3^l formation: *1* – channel; *2* – delta plain; *3* – delta front; *4* – shore–shallow lake; *5* – slope wash facies; *6* – well; *7* – floodplain; *8* – valley location; *9* – interdistribution bay; *10* – reverse trough fault breaking range; *11* – fan range.

Sedimentary system distribution characteristics in Es_3^l. The sedimentary environment of the Es_3^l unit was characterized by the development of a fan deltaic plain, a fan deltaic front, and the shore–shallow lake subfacies. In Es_3^l, the RMS amplitude attribute slice clearly depicted the boundary of the fan deltaic body (Fig. 6*a*). Moreover, as can be seen in Fig. 6, there was a small sediment supply capacity from the source area during the sedimentation period of the Es_3^l unit in this study area. Consequently, the fan delta spatial extent was restricted, and the development scale of river sand bodies was relatively small. During this period, the main sediment source was from the west (Fig. 6*b*).

Sedimentary system distribution characteristics in Es_3^u. The Es_3^u unit was found to develop mainly a fan deltaic plain, a fan deltaic front, and the shore–shallow lake subfacies. In Fig. 7*a*, the RMS amplitude attribute in green represents thicker sandstone, while blue represents thinner sedimentary sandstone. The boundary of the fan delta was delineated according to the thickness of the attribute slice, and the internal microfacies were finely delineated based on logging data. The Es_3^u unit in the research area exhibited significant development of fan deltas, on a relatively large scale. The main source direction of sediment supply for these fan deltas is from the west. Additionally, the development of river sand bodies in this unit was clearly evident; it was also characterized by a relatively large scale (Fig. 7*b*).

Paleogeomorphology. The Shulu Slope formed during the late Mesozoic to early Tertiary period, through gradual division against the background of regional uplift. Previous studies have shown that the Eocene Period was a warm period, during which precipitation increased (i.e., from dry to wet), leading to a transition of the lake surface from shallow to deep (Wu et al., 2017; Sun et al., 2022), during which the lake level rose from Es_3^l to Es_3^u. However, the well data in this study area show that the lake level in Es_3^u is deeper than that in Es_3^l (Figs. 8, 9), indicating that the distribution of ancient landforms caused by the structure in this area is the main factor controlling the sedimentary characteristics of the source-to-sink system, while climate and lake level changes under its influence are secondary factors.

During the sedimentation period of the Es_3 unit, the structural conditions of the Shulu Slope were relatively stable, and the ancient geomorphologic characteristics had a significant impact on its S2S elements. The width of the slope zone was small, and the main structure exhibited an upward tilt. Under the condition of a steep formation slope, gravity detachment may have occurred, causing the Shulu Slope shovel fault in the Jizhong Depression of the OBBB to slide gradually downward along the slope, which led to detachment.

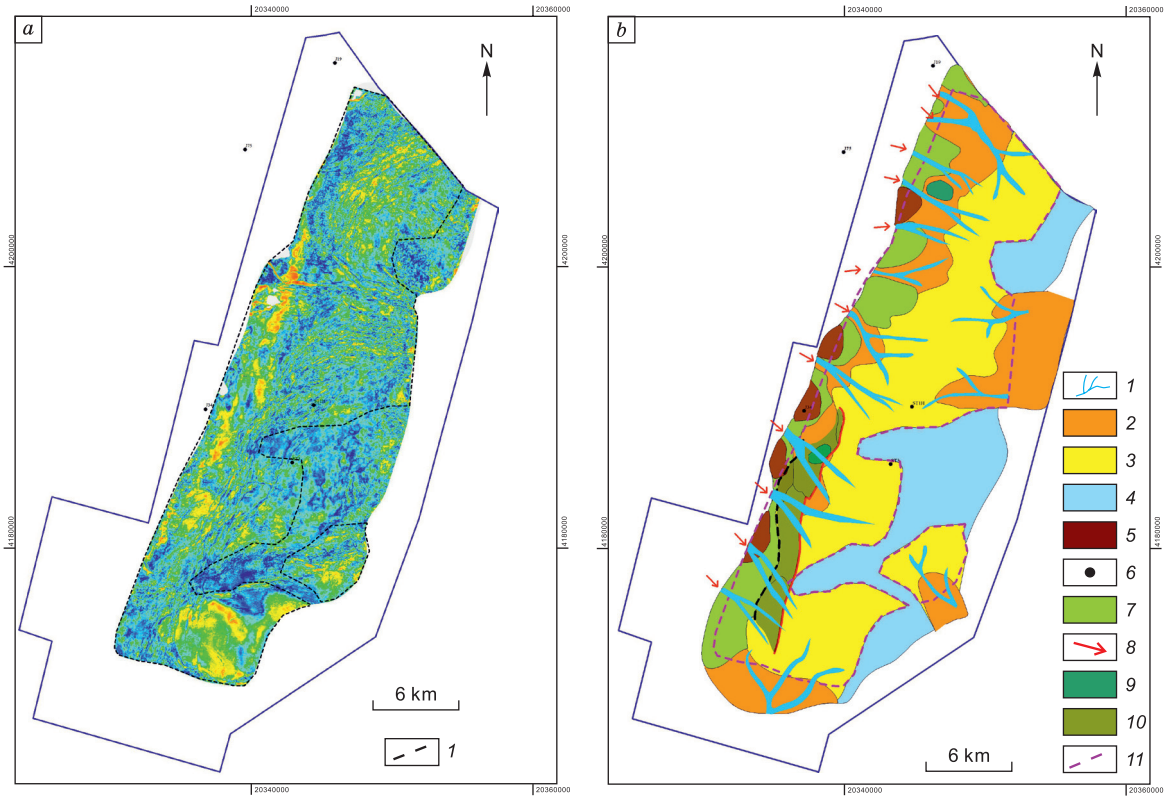

Fig. 7. Sedimentary distribution map of Es_3^u:

a – RMS amplitude attribute slice of the Es_3^u formation; *b* – sedimentary microfacies distribution map of Es_3^u. See legend in Fig. 6.

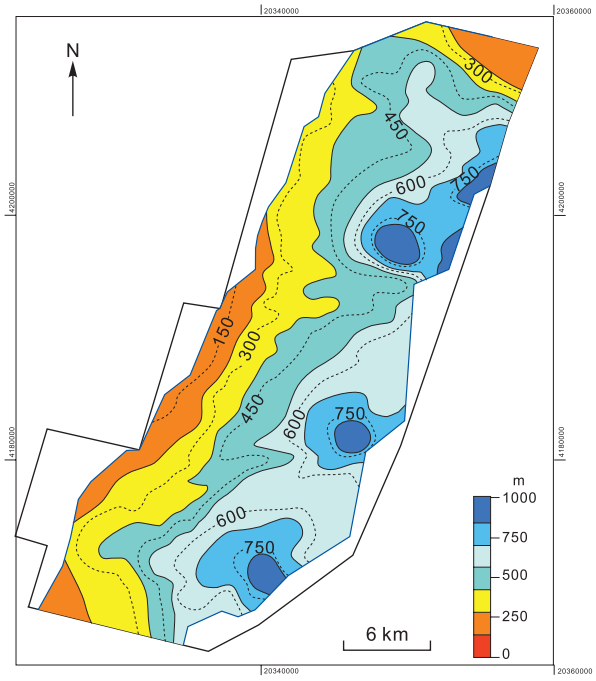

Fig. 8. Paleogeomorphology map of Es_3^l.

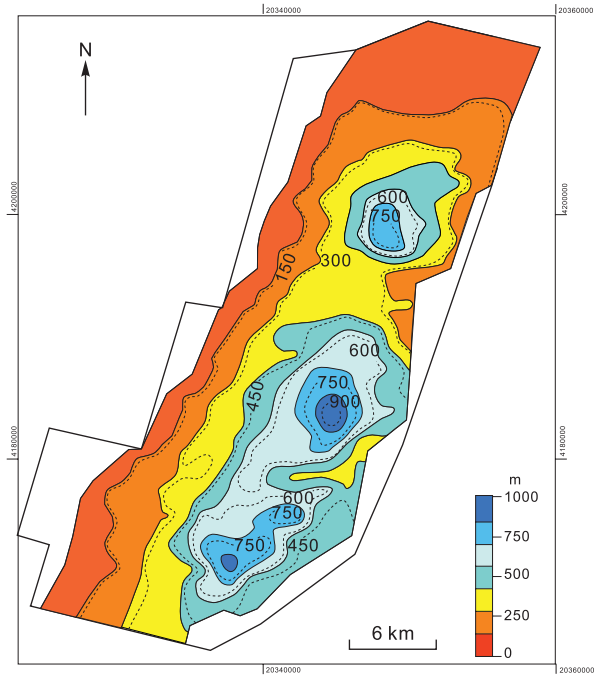

Fig. 9. Paleogeomorphology map of Es_3^u.

Under slopes with different terrains, debris exhibits varying transport ability, and the selective deposition of debris occurs under the influence of ancient landforms. The Shulu Slope, with its steep gradient, facilitates higher energy in the transport of detrital material. With a continuous supply of material sources, near-source sediment accumulates rapidly, leading to the smaller distribution area of the fan body compared to that of the gentle slope zone.

During Es_3^l (Fig. 10), the terrain in the northwest was low, while the terrain in the west remained higher. The fault trough was not developed, so sediment was transported mainly along valleys and distributed below

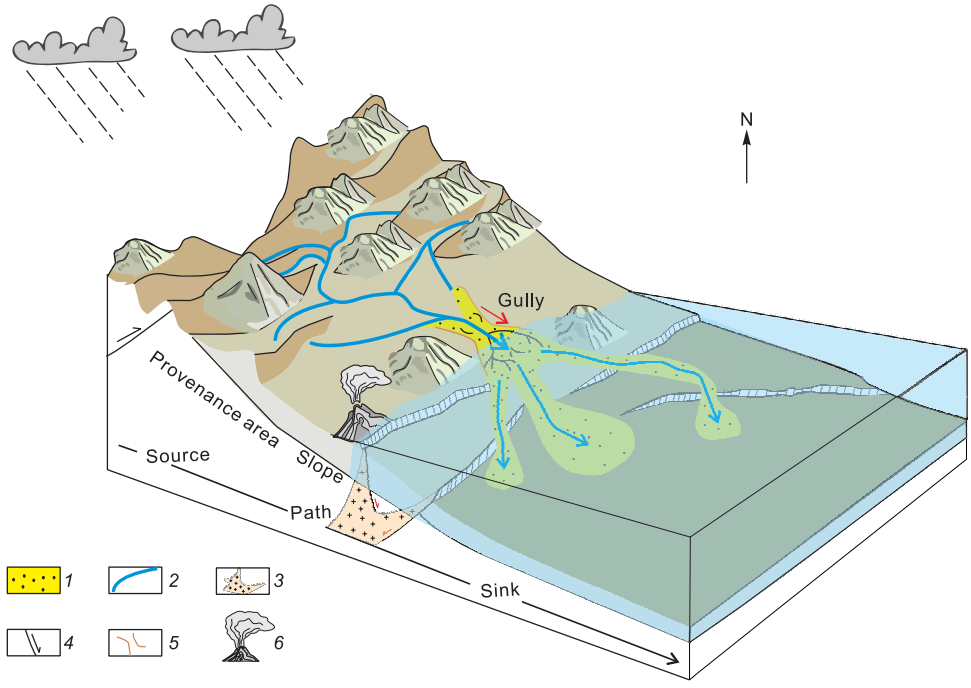

Fig. 10. Coupling mode of the source-to-sink system in Es_3^l:

1 – sand; *2* – channel; *3* – hydrothermal; *4* – fault; *5* – paleovalley; *6* – volcanic.

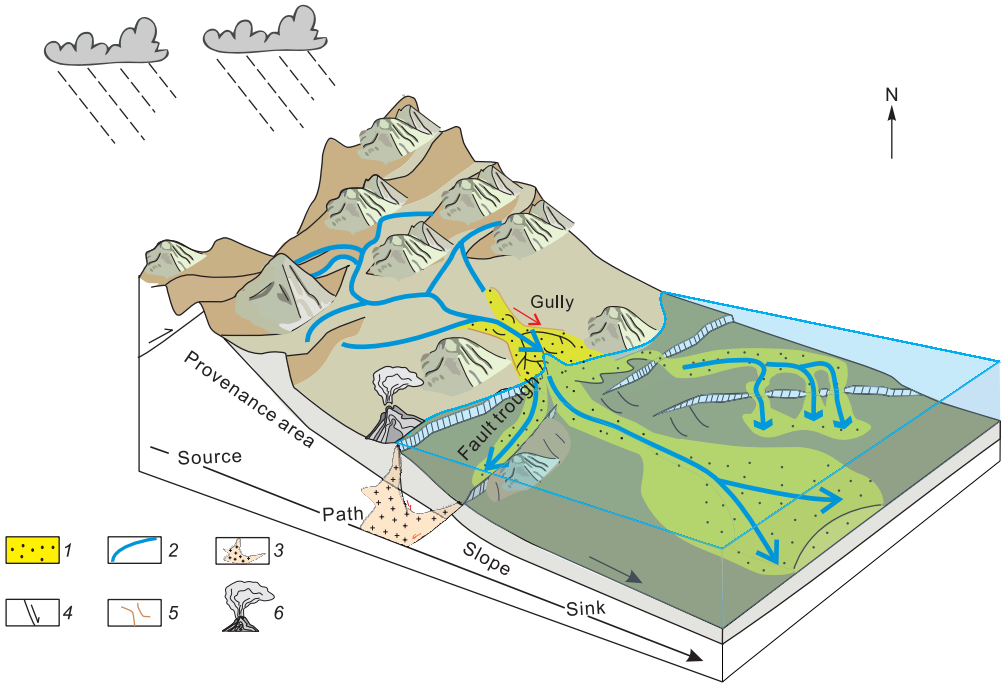

Fig. 11. Coupling mode of the source-to-sink system in Es_3^u.

See legend in Fig. 10.

the ancient valley. The ancient geomorphology of the Es_3^u (Fig. 11) is characterized by the higher elevation on the western side, while that on the eastern side is lower with a developed fault trough in the middle of the slope. Sediment entering the study area from the west is transported along the fault trough and distributed at the end of the slope.

S2S coupling mode. In the Es_3, the Shulu Slope is characterized by a steep terrain, with the provenance area being the Ningjin Uplift. The ability to provide sediment varies through different evolutionary periods, influenced by landforms and lake levels, and weathering and denudation products from the source area of the Ningjin Uplift were transported to the end of the slope through valleys and fault troughs.

During the sedimentation period of Es_3^l, the lake level was relatively low, and the debris material from the west gradually discharged along the ancient valleys and spread below them. During the sedimentation period of Es_3^u, the climate became humid, but under the influence of tectonic uplift, the lake level lowered. Clastic materials from the western Ningjin Uplift were transported through ancient valleys and fault channels and gradually unloaded along the slope, which resulted in the formation of a large-scale fan delta in this study area. Finally, an S2S model was proposed for the subfacies sedimentation of the Ningjin Uplift, including sand supply, fault trough, valley migration, fan delta, and shallow lake. This model has universal applicability and has guiding significance for predicting large-scale sand bodies in areas, such as the steep slope area of the Jiyang Depression in the Bohai Bay Basin (Gao et al., 2024), the slope zone of the Ulyastai Depression in the Erlian Basin (Feng et al., 2021), the western slope of the Mahu Depression in the Zhungeer Basin (Xiao et al., 2021), and the steep mountain range area of the Baikal Rift System (Byzov and Sankov, 2024).

CONCLUSIONS

(1) The geologic features and lithologic properties of the ancient OBBB environment suggest that the primary source of material at the research site is from the west. Previous studies have identified the Ningjin Uplift in the western region as the primary source area for the material found in this study area;

(2) Two types of sand transport trajectories developed in the Es_3 of the Shulu Slope, among which Es_3 developed valleys and fault troughs, while Es_3^l developed only valleys. Their seismic characteristics indicate that the valleys that developed in Es_3 are of inherited nature;

(3) Based on the characteristics of the S2S system elements, an S2S coupling model has been proposed, namely, "The Ningjin Uplift sand supply–fault trough, valley transport–fan delta, and shore–shallow lake subfacies sedimentation."

This study was supported by the National Natural Science Foundation (Nos. 42002153, 42102173, and 42172161), the Heilongjiang Philosophy and Social Science Foundation (No. 22EDE389), the China Postdoctoral Science Foundation (No. 2021M691193), and the Jilin Province People's Government Department of Education (No. JJKH20211111KJ).

REFERENCES

Bergal-Kuvikas, O.V., Buslov, M.M., Bushenkova, N.A., Dolgaya, A.A., 2023. Transition from the continental margin of Kamchatka to the island arc of the Kurile Islands: Features of volcanism, crustal deformation and geophysical parameters of the slab. Russ. Geol. Geophys. 64, 1227–1240, doi: 10.2113/RGG20234558.

Byzov, L., Sankov, V., 2024. The evolution of continental rifts revealed from the numerical modeling: A case study of the Baikal rift system, Siberia. J. Asian Earth Sci. 259, 105871, doi: 10.1016/j.jseaes.2023.105871.

Cai, C., Qiu, N.S., Liu, N., Li, Z.M., Wang, Y.J., Yu, Z.W., Gao, T., Jiao, Y.X., 2022. Geochemistry of formation waters and crude oils in the Shulu Sag, Bohai Bay Basin, NE-China, to assess quality and accumulation of hydrocarbons. J. Pet. Sci. Eng. 210, 110057, doi: 10.1016/j.petrol.2021.110057.

Cuitiño, J.I., Bilmes, A., Buono, M.R., Bordese, S., Herazo, L., Scasso, R.A., 2023. Stratigraphy, provenance, and timing of Neogene sedimentation in the western Valdés Basin, Patagonia. Accurate paleogeographic reconstructions as a key piece for andean-passive margin integration. J. South Am. Earth Sci. 124, 104278, doi: 10.1016/j.jsames.2023.104278.

Devyatov, V.P., Nikitenko, B.L., 2023. Stratigraphy and sedimentogenesis of the clinoform Upper Jurassic of the Anabar–Lena sedimentary basin (Arctic Siberia, Laptev Sea coast). Russ. Geol. Geophys. 64, 1347–1357, doi: 10.2113/RGG20234620.

Eliseev, A.A., Metelkin, D.V., Abashev, V.V., Mikhaltsov, N.E., Vinogradov, E.V., Bragin, V.Yu., 2024. Paleomagnetism of the Abinskaya Group of the Kuznetsk Depression (southern Siberia) – Implications for the evolution of the Siberian Large Igneous Province at the Permian–Triassic boundary. Russ. Geol. Geophys. 65, 475–490, doi: 10.2113/RGG20234692.

Feng, W.P., Wang, F.Y., Shi, Y.L., Jiang, T., Wang, Y.F., Zhou, H.F., Ma, X.F., Ma, Y., Pang, Q.J., 2021. Oil properties variation among the China Erlian Rift Basin petroleum systems: Correlation with organofacies and maturity. Mar. Pet. Geol. 127, 104960, doi: 10.1016/j.marpetgeo.2021.104960.

Feng, Y.L., Jiang, S., Hu, S.Y., Li, S.T., Lin, C.S., Xie, X.N., 2016. Sequence stratigraphy and importance of syndepositional structural slope-break for architecture of Paleogene syn-rift lacustrine strata, Bohai Bay Basin, E. China. Mar. Pet. Geol. 69, 183–204, doi: 10.1016/j.marpetgeo.2015.10.013.

Gao, J.H., Liang, X.P., Jin, Z.J., Liu, Q.Y., Li, C.R., Huang, X.W., Shi, J.Y., Li, P., 2024. Impact of volcanism on the formation and hydrocarbon generation of organic-rich shale in the Jiyang Depression, Bohai Bay Basin, China. Pet. Sci., doi: 10.1016/j.petsci.2024.01.017.

Jiang, Z.X., Kong, X.X., Yang, Y.P., Zhang, J.G., Zhang, Y.F., Wang, L., Yuan, X.D., 2021. Multisource genesis of continental carbonate-rich fine-grained sedimentary rocks and hydrocarbon sweet spots. Pet. Explor. Dev. 48, 26–37, doi: 10.11698/PED.2021.01.03.

Kong, X.X., Jiang, Z.X., Han, C., Zheng, L.J., Zhang, Y.M., Zhang, R.F., Tian, J.Z., 2017. Genesis and implications of the composition and sedimentary structure of fine-grained carbonate rocks in the Shulu sag. J. Earth Sci. 28, 1047–1063, doi: 10.1007/s12583-016-0927-x.

Kong, X.X., Jiang, Z.X., Han, C., Li, H.P., Li, Q., Zheng, L.J., Yang, Y.P., Zhang, J.G., Xiao, F., 2019a. Sedimentary characteristics and depositional models of two types of homogenites in an Eocene continental lake basin, Shulu Sag, eastern China. J. Asian Earth Sci. 179, 165–188, doi: 10.1016/j.jseaes.2019.04.023.

Kong, X.X., Jiang, Z.X., Han, C., Zheng, L.J., Zhang, J.G., 2019b. The tight oil of lacustrine carbonate-rich rocks in the Eocene Shulu Sag: Implications for lithofacies and reservoir characteristics. J. Pet. Sci. Eng. 175, 547–559, doi: 10.1016/j.petrol.2018.12.028.

Kong, X.X., Jiang, Z.X., Han, C., Zhang, R.F., 2020. Organic matter enrichment and hydrocarbon accumulation models of the marlstone in the Shulu Sag, Bohai Bay Basin, Northern China. Int. J. Coal Geol. 217, 103350, doi: 10.1016/j.coal.2019.103350.

Kosenko, I.N., Pestchevitskaya, E.B., Efremenko, V.D., Metelkin, E.K., Yan, P.A., Rodchenko, A.P., Nikitenko, B.L., Mirzabaev, D.A., 2023. Turga Lagerstätte (Middendorf's outcrop, Eastern Transbaikalia, Barremian–Aptian): Stratigraphic range and palaeoenvironments. Russ. Geol. Geophys. 64, 1358–1381, doi: 10.2113/RGG20234625.

Li, Q., You, X.L., Jiang, Z.X., Wu, S.H., Zhang, R.F., 2020a. Lithofacies and reservoir characterization of a source-controlled carbonate succession in a lacustrine rift basin, the Shulu Sag of Bohai Bay Basin, East China. J. Pet. Sci. Eng. 192, 107180, doi: 10.1016/j.petrol.2020.107180.

Li, Q., You, X.L., Jiang, Z.X., Wu, S.H., Zhang, R.F., 2020b. The origins of carbonate minerals of a source-controlled lacustrine carbonate succession in the Shulu sag, Bohai Bay Basin: Implications for porosity development and paleoenvironment. Mar. Pet. Geol. 122, 104673, doi: 10.1016/j.marpetgeo.2020.104673.

Li, Y., Wang, S., Ye, Z., Lin, S., Wang, Y., Zuo, S., 2023. The sedimentary filling differences of subsags and their impacts on oil shale and coal accumulation in a rift lacustrine sag: A case study from the Lower Cretaceous in the Zhangqiang sag, southern Songliao Basin, Northeast China. Mar. Pet. Geol. 155, 106354, doi: 10.1016/j.marpetgeo.2023.106354.

Liang, J.T., Wang, H.L., Blum, M.J., Ji, X.Y., 2020. Modeling of hydrocarbon migration and accumulation on the Chengzikou uplift, Bohai Bay Basin, China: Implications for petroleum exploration on slope belts in rift basins. J. Pet. Sci. Eng. 189, 106963, doi: 10.1016/j.petrol.2020.106963.

Liu, H., Meng, J., Banerjee, S., 2017. Estimation of palaeo-slope and sediment volume of a lacustrine rift basin: A semi-quantitative study on the southern steep slope of the Shijiutuo Uplift, Bohai Offshore Basin, China. J. Asian Earth Sci. 147, 148–163, doi: 10.1016/j.jseaes.2017.07.028.

Liu, H.Q., Hong, Z., Zhang, J., Niu, H.Q., Li, S.W., Long, L.W., 2016. Sedimentary characteristics and seismic geomorphology of gravity-flow channels in a rift basin: Oligocene Shahejie Formation, Qinan Slope, Huanghua Depression of Bohai Bay Basin, China. Mar. Pet. Geol. 78, 807–825, doi: 10.1016/j.marpetgeo.2016.02.014.

Liu, L., Chen, H.D., Wen, H.G., Xu, W.L., Zhong, Y.J., Wang, X.L., Wang, Z.W., 2020. Facies architecture and sediment infilling processes in intrabasinal slope belts of lacustrine rift basins, Zhanhua Depression, Bohai Bay Basin. Mar. Pet. Geol. 112, 104089, doi: 10.1016/j.marpetgeo.2019.104089.

Liu, N., Qiu, N.S., Cai, C., Li, Z.M., Wang, Y.J., Jiao, Y.X., Gao, T., Sun, H.L., Lu, M., 2022. Geochemical characteristics and natural gas-oil-source correlation of the Shulu depression in the Jizhong Subbasin, Bohai Bay Basin, eastern China. J. Pet. Sci. Eng. 216, 110831, doi: 10.1016/j.petrol.2022.110831.

Liu, Q.H., Zhu, X.M., Zeng, H.L., Li, S.L., 2019. Source-to-sink analysis in an Eocene rifted lacustrine basin margin of western Shaleitian Uplift area, offshore Bohai Bay Basin, eastern China. Mar. Pet. Geol. 107, 41–58, doi: 10.1016/j.marpetgeo.2019.05.013.

Liu, Q., Li, P., Jin, Z., Sun, Y.W., Hu, G., Zhu, D.Y., Huang, Z.K., Liang, X.P., Zhang, R., Liu, J.Y., 2021a. Organic-rich formation and hydrocarbon enrichment of lacustrine shale strata: A case study of Chang 7 Member. Sci. China Earth Sci. 65, 118–138, doi: 10.1007/s11430-021-9819-y.

Liu, Q., Li, P., Jin, Z., Liang, X.P., Zhu, D.Y., Wu, X.Q., Meng, Q.Q., Liu, J.Y., Fu, Q., Zhao, J.H., 2021b. Preservation of organic matter in shale linked to bacterial sulfate reduction (BSR) and volcanic activity under marine and lacustrine depositional environments. Mar. Pet. Geol. 127, 104950, doi: 10.1016/j.marpetgeo.2021.104950.

Nemova, V.D., Shakhov, A.S., Bazhukova, T.A., Isangulova, A.M., Kim, O.O., Skomorokhova, A.D., 2024. Upper Jurassic sediments in the western side of the Frolovskoye basin in West Siberia: Diverse patterns and environments of deposition. Russ. Geol. Geophys., doi: 10.2113/RGG20234683.

Paisani, J.C., Pereira, J.S., Vinicius de Sordi, M., Manica, R., 2023. Pleistocene-Holocene colluvial facies from the Volcanic Plateau of the Paraná Sedimentary Basin (Rio Grande do Sul, Brazil) – sedimentation processes and paleoenvironmental implications. J. South Am. Earth Sci. 126, 104344, doi: 10.1016/j.jsames.2023.104344.

Peng, B., Jin, Z., Wang, J., Jia, H., Zhu, X., Chang, T., Yuan, K., 2018. Sedimentology and sequence stratigraphy of a retrogradational fan-delta system within Lower Triassic in the Mabei area, Junggar Basin (northwestern China). Russ. Geol. Geophys. 59, 606–619, doi: 10.1016/j.rgg.2018.05.002.

Polyansky, O.P., Simonov, V.A., Koroleva, O.V., Prokopiev, A.V., Babichev, A.V., Kotlyarov, A.V., Semenov, A.N., 2024. Two-stage model of Devonian basic magmatism in the Vilyui paleorift (Siberian Platform). Russ. Geol. Geophys., doi: 10.2113/RGG20234666.

Ribeiro, S.R., Valadão, R.C., Gomes, M.O.S., Bittencourt, J.S., Alves, R.A., 2023. Paleoecological indicators of the highstand sea level on the Amazonian supralittoral until the last two millennia. J. South Am. Earth Sci. 128, 104422, doi: 10.1016/j.jsames.2023.104422.

Savelyev, D.P., Palesskii, S.V., Portnyagin, M.V., 2018. The source of platinum group elements in basalts of the ophiolite complex of the Kamchatsky Mys Peninsula (Eastern Kamchatka). Russ. Geol. Geophys. 59, 1592–1602, doi: 10.1016/j.rgg.2018.12.005.

Sun, L., Zhang, J.L., Li, Y., Yan, X., Zhang, X.C., 2022. Paleosalinity and lake level fluctuations of the 3rd Member of Paleogene Shahejie Formation, Chezhen Sag, Bohai Bay Basin. Front. Earth Sci. 16, 949–962, doi: 10.1007/s11707-022-0979-0.

Tang, X., Zhang, J.C., Jiang, Z.X., Zhang, R.F., Lan, C.L., Zhao, W.S., Zhu, J.Q., Wang, J.M., Zhao, P.W., 2018. Heterogeneity of organic-rich lacustrine marlstone succession and their controls to petroleum

expulsion, retention, and migration: A case study in the Shulu Sag, Bohai Bay Basin, China. Mar. Pet. Geol. 96, 166–178, doi: 10.1016/j.marpetgeo.2018.05.031.

Tian, R.H., Xian, B.Z., Wu, Q.R., Shu, Q.L., Liu, J.P., Zhang, W.M., Wang, Z., Li, Q., Rahman, N.U., Gao, Y.K., Wang, J.W., 2023. Turbidite system controlled by fault interaction and linkage on a slope belt of rift basin: Zhanhua depression, Bohai Bay Basin, China. Mar. Pet. Geol. 155, doi: 10.1016/j.marpetgeo.2023.106377.

Travin, A.V., Buslov, M.M., Bishaev, Yu.A., Tsygankov, A.A., Mikheev, E.I., 2023. Late Paleozoic–Cenozoic tectonothermal evolution of Transbaikalia: Thermochronology of the Angara–Vitim granitoid batholith. Russ. Geol. Geophys. 64, 1086–1097, doi: 10.2113/RGG20234577.

Velivetskaya, T.A., Ignatiev, A.V., Vysotskiy, S.V., Aseeva, A.V., 2024. Ratios of sulfur isotopes (^{32}S, ^{33}S, ^{34}S, and ^{36}S) in Archean rocks of Karelia: Evidence of microbial life and the anoxic atmosphere. Russ. Geol. Geophys., doi: 10.2113/RGG20234602.

Wang, T., Yuan, S.Q., Li, C.X., Mao, F.J., Pang, S.C., Jiang, H., Zheng, F.Y., 2022. Geological structure and dynamic mechanism of the Termit rift basin in West African rift system. Pet. Explor. Dev. 49, 1339–1350, doi: 10.1016/S1876-3804(23)60353-2.

Wu, L.J., Wang, F.K., Wang, D.H., Fu, M., Jia, Y.H., 2017. The lithologic differences between the third and fourth members of the Eocene Shahejie Formation in the Bohai Bay Basin and the associated climatic evolution. Geol. J. 53, 788–802, doi: 10.1002/gj.2927.

Xiang, P.F., Ji, H.C., Shi, Y.Q., Du, Y.B., Chen, P., Weng, Q.P., Xu, X.R., Sun, Y.S., Huang, Y., Zou, S.Q., 2021. Characteristics and formation mechanism of mesogenetic dissolution: A case study of Ordovician carbonate in the western slope of the Shulu Sag, Jizhong Depression, Bohai Bay Basin. J. Pet. Sci. Eng. 206, 109045, doi: 10.1016/j.petrol.2021.109045.

Xiao, Z.L., Chen, S.J., Liu, C.W., Lu, Z.X., Zhu, J., Han, M.M., 2021. Lake basin evolution from early to Middle Permian and origin of Triassic Baikouquan oil in the western margin of Mahu Sag, Junggar Basin, China: Evidence from geochemistry. J. Pet. Sci. Eng. 203, 108612, doi: 10.1016/j.petrol.2021.108612.

Zhao, L., Mao, W., Liu, Z., Cheng, S., 2023. Research on the differential tectonic-thermal evolution of Longmaxi shale in the southern Sichuan Basin. Adv. Geo-Energy Res. 7, 152–163, doi: 10.46690/ager.2023.03.02.

Zhao, X.Z., Li, Q., Jiang, Z.X., Zhang, R.F., Li, H.P., 2014. Organic geochemistry and reservoir characterization of the organic matter-rich calcilutite in the Shulu Sag, Bohai Bay Basin, North China. Mar. Pet. Geol. 51, 239–255, doi: 10.1016/j.marpetgeo.2013.12.014.

Zhao, X.Z., Jin, F.M., Li, Y.B., Wang, Q., Zhou, L.H., Lyu, Y.F., Pu, X.G., Wang, W., 2016. Slope belt types and hydrocarbon migration and accumulation mechanisms in rift basins. Pet. Explor. Dev. 43, 915–924, doi: 10.1016/S1876-3804(16)30110-0.

Zheng, L.J., Jiang, Z.X., Liu, H., Kong, X.X., Li, H.P., Jiang, X.L., 2015. Core evidence of paleoseismic events in Paleogene deposits of the Shulu Sag in the Bohai Bay Basin, east China, and their petroleum geologic significance. Sediment. Geol. 328, 33–54, doi: 10.1016/j.sedgeo.2015.07.013.

Zhu, C.Z., Gang, W.Z., Li, X.F., Wang, N., Guo, Y., Zhao, X.Z., Wang, Y.F., Pu, X.G., 2022. The sorting effect of hydrodynamics on the geochemical compositions of sedimentary organic matter in a lacustrine rift basin: Significance for hydrocarbon exploration on the Qibei slope, Bohai Bay Basin, China. Mar. Pet. Geol. 141, 105705, doi: 10.1016/j.marpetgeo.2022.105705.